

# CFD Analysis of Viscous Flows in the Sharp Corner of the Grid Fins

Chiranjeevi Sadana<sup>1</sup>, Sridhar B.T.N.<sup>2</sup>

<sup>1</sup>Student, Department of Aerospace Engineering, MIT Campus, Anna University, Chennai, India

<sup>2</sup>Anna University, Chennai, India  
2017612004[at]annauniv.edu.in, sridhar[at]mitindia.edu

**Abstract:** The objective of the present study is to verify the flow features including Shock- Shock interactions, Shock-Boundary layer interactions in the sharp corners of the grid fins at free stream Mach numbers 0.8,1.2,1.8,2,2.5, and 3 for the grid fin with chord length 70mm and the gap length 70 mm and thickness 4mm with sharp leading edge and tailing edge. The most important outcome of the 2D studies was idea of classification of different flow regimes encountered in supersonic flow past series plates namely Single body regime, Single Plate regime, Separated Flow regime. These basic flow regimes explain in the Mach 2 flows can be readily extended to higher supersonic flows without any effects. Numerical analysis was also carried out for 3D grid fin single cell with SST turbulence model. First cell height was provided with 5 microns so that maximum  $Y^+$  will be less than 1. The different regimes mentioned in the 2D results were also realized in the 3D results. For Mach number 2 and 2.5, The shock -shock boundary layer interactions region was identified and for Mach 3 it was observed that grid fin cell was free from these interactions. Further, Velocity profiles were extracted at different stations along the sharp corner of the grid-fin cell to identify the important flow phenomenon like flow separation, Displacement thickness and Momentum thickness. The boundary layer development and growth along the sharp corner and on the flat surface of the grid fin flow were compared and analyzed. The rate of boundary layer growth and boundary layer thickness were higher along the sharp corner when compared to those on flat surface.

**Keywords:** Gridfin Flow, CFD Analysis, Boundarylayer

## 1. Introduction

The grid fin is a unique device that can be used as either an aerodynamic stabilizer or a control surface. Its unique design and aerodynamic characteristics separate it from conventional planar fins. Planar fins can generally be described in (DİKBAŞ, 2015) with information about the root chord, tip chord, span and thickness. Grid fins however possess an extra dimension. Grid fins require five geometric parameters to describe their geometry (span, chord, height, cell spacing and element thickness). Different theoretical formulations were used in (DİKBAŞ, 2015) for the subsonic, transonic, and supersonic flow regimes due to the drastically different flow fields that the grid fin experiences in each Mach regime. These simulations use a vortex lattice approach in the subsonic and transonic flow regimes, with a correction factor that is applied in the transonic flow regime to account for mass flow spillage due to the choking of the flow within each individual cell of the grid fin. Recent studies and experimentations show that grid fins can be used in launch vehicles for various purposes including in crew escape system, stage recovery. The purpose of this work is incorporate the CFD analysis of viscous flows in the sharp corner of the grid fin cell at free stream Mach numbers 0.8,1.2,2,2.5,3. CFD analysis was carried out to understand the basic flow features like shock interactions, shock- shock interactions, shock-shock-boundary layer interactions, flow separation region in the grid fin cells by considering the cross-sectional section by keeping the geometric parameters constant. 2D CFD analysis was carried out for the free stream Mach numbers 0.8, 1.2 and 2. The work was carried out using

the numerical approach in which Ansys Fluent was used as a tool.

The outcome of the present work can be used to identify the Mach number regions where the shock impinges on the surface of the grid fin and Mach number in which grid fin cell is free from the shock impingements and this can be used as reference for the grid fin flows. If there is restriction in the dimensions of the grid-fin further technologies need to asses to make the flow to attach on the wall surface by the suction methodologies.

## 2. Model Geometry

Dimensions of the grid fin consists of distance between sharp leading edge and sharp tailing edge is 70mm and thickness  $t$  4mm. Distance between the grid fins called width  $w$  which is 70mm.

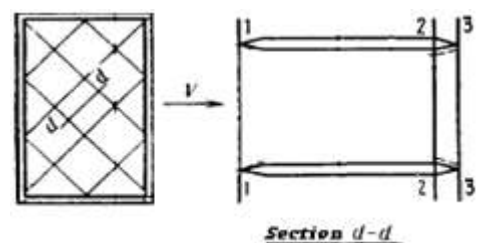


**Figure 1:** Grid Fins and Cross section from the (DİKBAŞ, 2015)

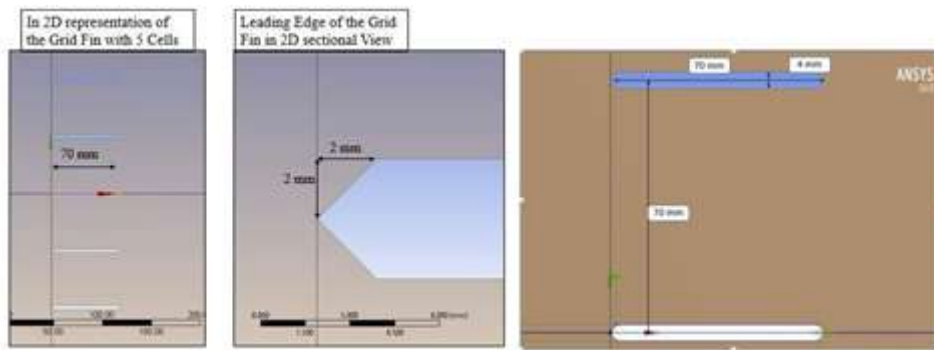


Figure 2: Geometry specifications of the current model

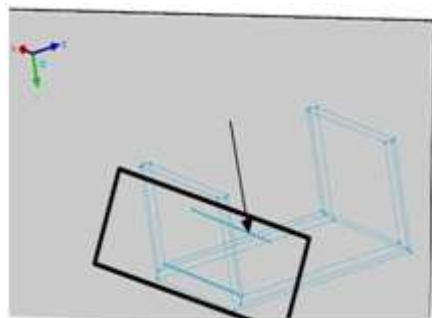


Figure 3: Corner Region of the 3D Grid Fin Cell

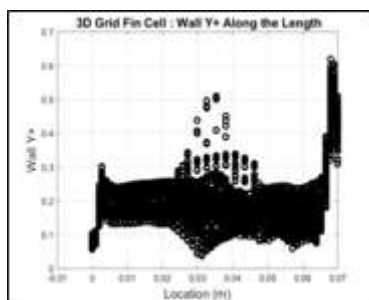


Figure 4: Wall Y+ along the sharp corner of grid fin

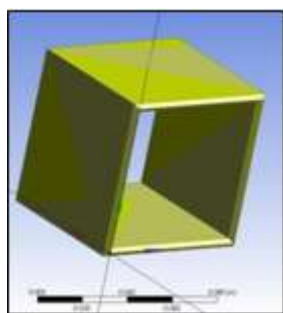


Figure 5: 3D Grid Fin Single Cell

### 3. Methodology

Numerical analysis was carried out initially for the grid fin 2d section consisting of 5 cells at free stream Mach numbers 0.8, 1.2 and 2 using Spalart–Allmaras turbulence model since the flow was considered fully turbulent Initial parametric study was carried out for chord length ranging from 10mm to 70mm within steps of 10mm at free stream Mach numbers 0.8, 1.2, 2. Further, numerical analysis was carried out for the 70mm chord length at angles of attack  $4^\circ$ ,  $8^\circ$ ,  $12^\circ$  and  $16^\circ$  by keeping gap length and thickness constant. Boundary layer was captured very well with maximum Y+ value 0.5. Viscous padding was carried out with 25 prism

layers on the wall with growth rate 1.2. Two separate grids were constructed for the freestream Mach number 2, with 0.219 million cells and 139996 nodes. In case of freestream Mach numbers 1.2 and 0.8, the mesh consisted of 2 million cells and 1175283 nodes. All triangular cells were used outside the viscous padded layers and inside tetra cells were used. Fluent solver was used to solve Navier-Stokes equations. Convergence criterion was set for the residuals at  $1 \times 10^{-4}$ . Grid independence study was carried for 3 different grids in which error percentage in the  $C_d$  and  $C_n$  values were within 2%.

Computational Domain for CFD Simulations

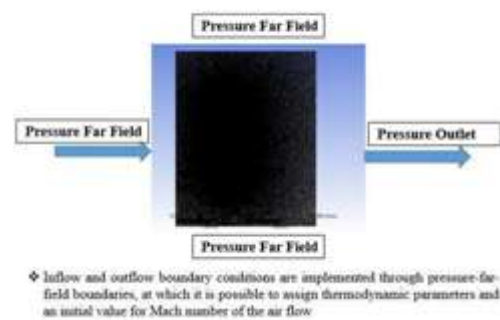


Figure 6: Methodology using in the CFD analysis

Computational Fluid Dynamics (CFD) is the major method to predict the aero-dynamic forces exerted on grid fin. ‘Single Grid Fin Cell’ approach is employed to make solutions accessible for the flow features inside the cell.

CAD models are created in ANSYS Design Modeler package. Parametric design option is helpful in reproducing the models of different dimensional properties. Cylindrical enclosure volume, which has minimum ~20 times greater diameter and length dimension, is created to represent the flow domain. The aerodynamic model is located at the center of enclosure volume. ANSYS 19.2 meshing tool is employed to generate unstructured grids. For all geometric configurations of grid fin geometry, surface mesh consists of triangular elements in order to ease the production of high-quality cells. Prism layers are grown starting from the surface for the purpose of resolving the high velocity gradients in boundary layer. In order to fill the remaining volume of the domain, tetrahedral cell elements are generated. As a result, computational domain is composed only of wedge and tetrahedral cells. Density-based Reynolds Averaged Navier-Stokes solver of FLUENT 19.2 is utilized throughout the study. Ideal gas assumption is selected as equation of state for air flow. Viscosity-temperature relation is characterized by Sutherland’s law. One equation Spalart-

Allmaras model is utilized as the turbulence model. Momentum and energy equations are discretized by second order upwind scheme in order to obtain more accurate results for estimation of drag. Coupled algorithm of FLUENT solver is employed to make the simulations converge faster.

### 3.1 Validation Study of Computational Method

The validation study carried out by (Krishnamurthy, Shende, & Narayanarao, 2013) 2D geometry provided similar boundary conditions and turbulence models and almost same grid size to compare the results with the Fluent solver and HiFun Solver.

The configuration considered in the validation study with an objective of understanding the flow physics, involves an idealized grid-fin configuration, represented by finite series of plates. These computations are essentially two dimensional in nature. For the series of plates in 2D, 5 Plates each of length 50 mm and 10mm thickness were stacked one above the other with spacing of 50 mm. (Krishnamurthy et al., 2013) was considered 3D isolated grid fin configuration with 4x3 grid where each cell is a 50mm cube with the plate thickness being 10mm. Here the leading and trailing edges of the plates, unlike in 2D configuration are blunt.

### 3.2 Grid Construction for the 2D Model

Two fine unstructured grids, Grid1 for high Mach number computations and Grid with a larger domain for transonic flow computations were generated for a series of plates. Total numbers of Field nodes for Grid1 were 90510 and Elements were 161583. Numbers of layers in viscous padding were 23 with First layer height being  $2 \times 10^{-2}$  mm with growth rate 1.1 from the surface of the grid fin. The extent of the domain in upstream provided 1.5c and in normal direction provided 50c and downstream provided with 50c where c is chord length being 50mm. All triangular elements were constructed outside the boundary layer and quad mesh was constructed inside the boundary layer. The quality of the mesh was very good is in the order of 0.31 in the orthogonal quality scale of 0 to 1 where 1 being super quality and 0 being poor quality

### 3.3 Computation

The CFD analysis carried out in the Fluent with modified Reynolds Average Navier Stokes equations using the

Spalart–Allmaras turbulence model considering fully turbulent in free stream flow. The boundary conditions specified as follows as Upstream, Top and Bottom considered as Far Field where provided with the Mach number and Static Pressure and Temperature at the altitude of the 3 kms of standard atmosphere model. Ideal gas assumption for the real flow and Sutherland law for temperature viscous model. Iterations were stopped until the convergence achieved with the residuals reach at  $10^{-5}$ . Similarly, computations carried out for the Mach 1.2, Mach 0.8. For Mach 2 further computations at different angle of attacks carried out.

### Boundary Layer Thickness, Displacement Thickness and Momentum Thickness

Boundary layer thickness was calculated using the literature that location at which velocity in the local station is equal to 99% of the freestream velocity. At a selected station boundary layer thickness identified based on the free stream velocity. Another consideration was also included by assuming that the flow inside the grid fin is completely similar to the pipe flow where the maximum velocity being at the centre of the grid fin. By considering the maximum velocity in the local station boundary layer thickness was identified. Displacement thickness and Momentum thickness was calculated using the formulae from (Schlichting & Gersten, 2016)

$$\delta^* = \int_0^{\delta} \left(1 - \frac{\rho u}{\rho_{\infty} u_{\infty}}\right) dy \quad (1)$$

$$\theta = \int_0^{\delta} \frac{\rho u}{\rho_{\infty} u_{\infty}} \left(1 - \frac{u}{u_{\infty}}\right) dy \quad (2)$$

Integrand values have been calculated locally in small elemental steps in a station and Summation carried out for all the Integrands which gives the Integral values of the displacement thickness and momentum thickness.

### 3.4 Grid Independence Study

Grid independence study carried out for the 2-D grid fin section with chord length 70mm. Three different grids were constructed based on the minimum length of the cell.

Free Stream Mach 2							
Alpha 0°							
Element Size	Number of Elements	Cells	% Change in Cells	C <sub>d</sub>	C <sub>l</sub>	Change in %	Change in %
0.2 mm	386049	Increase	24.6209678	0.42	-0.003		-1.351
0.4 mm	291000			0.4144	-0.005		
0.8 mm	121434	Decrease	58.27010309	0.41	-0.006		1.062
Alpha 4°							
Element Size	Number of Elements		% Change in Cells	C <sub>d</sub>	C <sub>l</sub>		
0.2 mm	386049	Increase	24.6209678	0.4244	1.0789	2.206	-2.413
0.4 mm	291000			0.4144	1.1027		
0.8 mm	121434	Decrease	58.27010309	0.4133	1.0828	1.805	0.265

Figure 7: Grid Independence study



Grid1 consist of the minimum length of the cell is 0.2mm, Grid2 consists of the minimum length of the cell is 0.4mm and Grid3 consists of the minimum length of the cell is 0.8mm. **Figure 7** illustrated the overall idea of the grid independence study for the current 2-D grid fin section.

to the shape of the geometry. The amount of acceleration is huge in the top windward and bottom leeward plates. Thin region very close to the wall can be seen which depicts the uniform boundary layer and further downstream is followed with little deflection due to the sharp edge i.e. flow turning away from itself.

**4. Results**

**Validation Results**

Validation study has been carried out for the  $C_l$  versus angle of attack for the model from the (Krishnamurthy et al., 2013) From the **Figure 8** it can be observed that CFD results for the *Fluent* solver and *HiFun* solver agree well with the theoretical values.

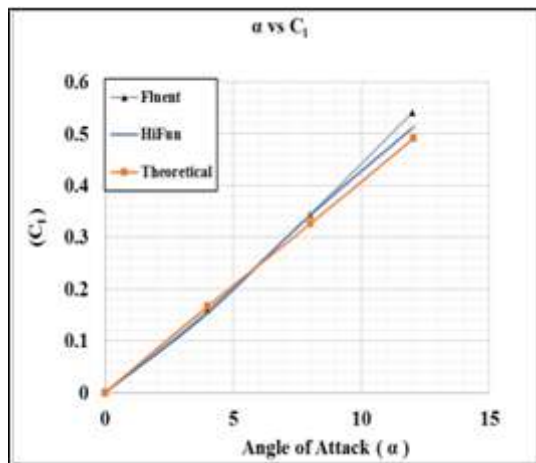


**Figure 8:** CA for 5 panels of different chord lengths

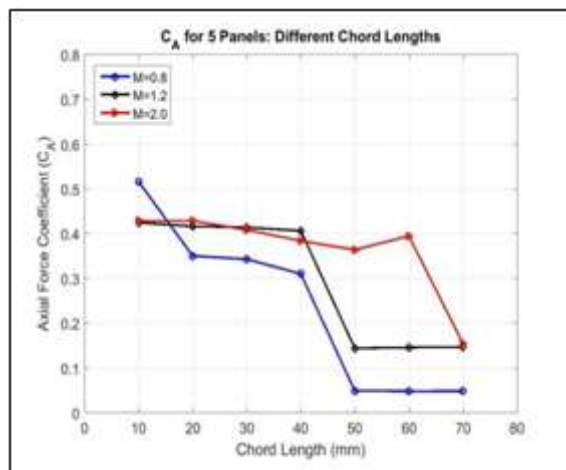


**Figure 9:** Validation results of the Coefficient of Lift Data

**Parametric Study on 2-D Section with Five Cells**

Numerical analysis was carried out initially for the grid fin 2d section consisting of 5 cells at free stream Mach numbers 0.8, 1.2 and 2 using Spalart–Allmaras turbulence model, since the flow was considered fully turbulent, Initial parametric study was carried out for chord length ranging from 10mm to 70mm with steps of 10mm at free stream Mach numbers 0.8, 1.2, 2. The results of this parametric study helped to understand the basic flow features inside the grid fin cell by differentiating the various regions. This can be observed in the **Figure 10**, **Figure 11**, **Figure 16** which shows grid fin flow in 2D at Mach number 0.8, 1.2 and 2 respectively. The flow is accelerating at the leading edge due

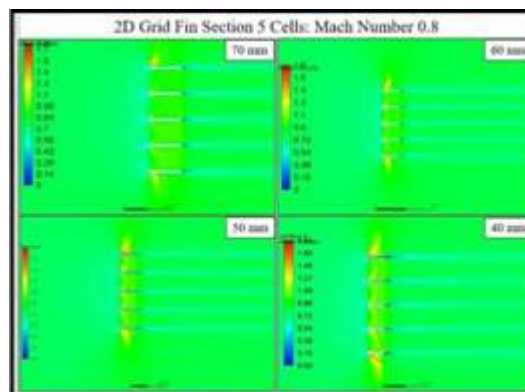


**Figure 10:** Parametric Study for 2D Plates at Mach 0.8

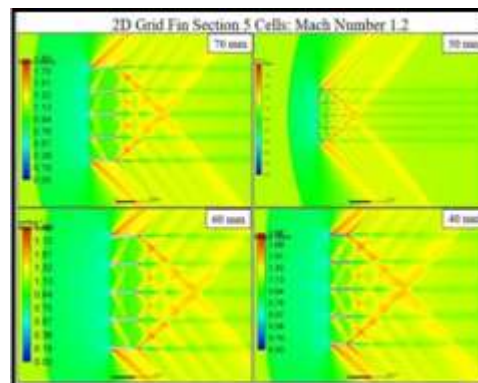


**Figure 11:** Parametric Study for 2D Plates at Mach 1.2

**Results for Freestream Mach Number 0.8**

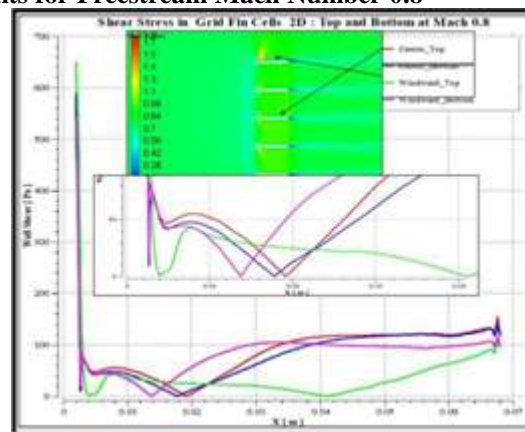


**Figure 12:** Wall Shear Stress Distribution in the 2D section in Mach 0.8 flow

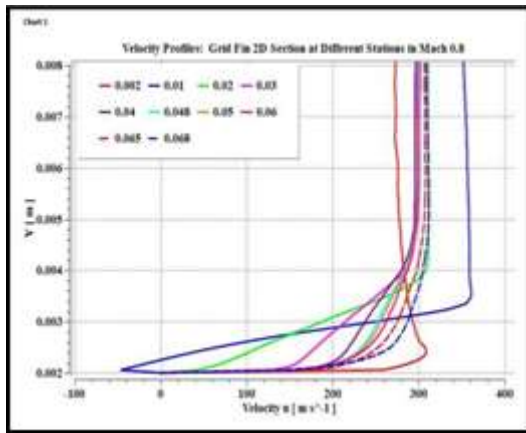


Figure 13: Velocity profiles at different stations in 2D section in Mach 0.8 flow

The strength of the sonic packets emanated from the leading edge of the section increases as the chord length decreases and further it is acting as a blockage to the upstream. From the Figure 9 it can be seen that the axial force coefficient was higher for the smallest chord length i.e., 10mm. Flow

became unstable at the beginning of the tailing edge due to the geometry can be seen from the Figure 12 for 0.068 location velocity profile showing non positive number.

**Results for Free Stream Mach Number 1.2**

Transonic Flow typically ranges from the Mach number in between 0.8-1.2. It has been observed from the Mach palette that the flow established further in downstream with strong Mach number compared to M=0.8. In Subsonic regime, flow started to accelerate due to the presence of the wedge in both normal directions from the wall. Due to decrease in the available area (formation of boundary layer) for the flow within the grid fins, flow acceleration can be observed from the Figure 15. But in the M=1.2 flow, a strong bow shock standing at a certain distance from the body which covers full geometry results in complex flow in downstream with full of reflections. These reflections act as a strong obstruction to the flow which was termed as the Bucket formation in the (Krishnamurthy et al., 2013).

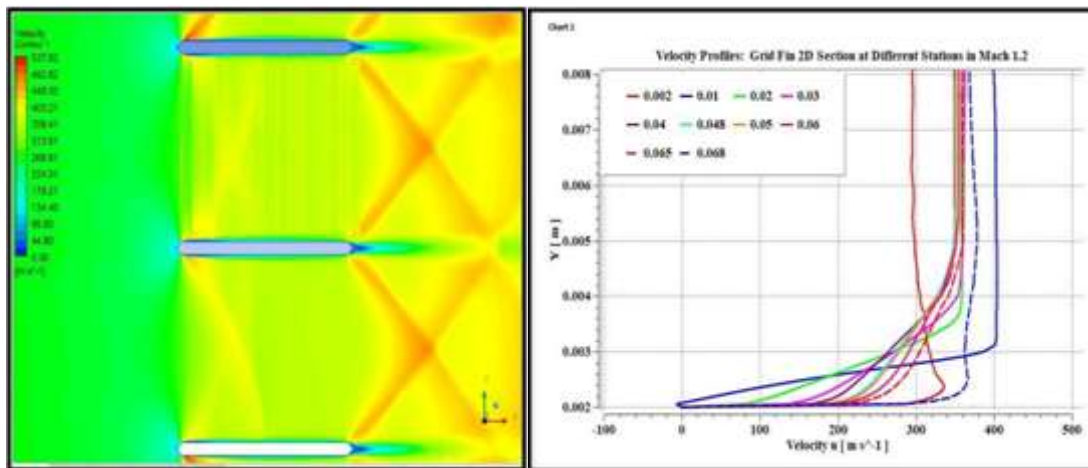


Figure 15: Velocity profiles for Grid Fin 2D section at different stations in Mach 1.2

Figure 15 represents the flow field in the Grid Fin 2D section for the Mach number 1.2. A bow shock wave is formed in front of the body, behind this shock wave the flow is locally subsonic. The pockets of the supersonic flow over top and bottom surfaces which can be seen and these were terminated by weak shock waves behind which the flow becomes subsonic again. This subsonic flow subsequently expands to low supersonic flow over the surface of the grid fin. Further increase in the freestream Mach number causes strengthening of these pockets of supersonic flow. These supersonic pockets hit the surface of the grid fin and become driving factors for the flow between the surfaces of the grid fin. This is further responsible for the flow in the downstream.

length 40mm to 20mm. However, the complex nature of the flow increases for the shorter chord length resulting high wave drag.

Results of the parametric study indicate that the possible candidate for the grid fin configurations for gap length 70mm may be with the chord length 70mm containing low CA value in the Mach numbers 0.8, 1.2 and 2.

**Results for Freestream Mach Number 2**

The contours of Mach number for the parametric study of freestream Mach 2 has been given in the Figure 16. The shock impingement location on the top surface of the grid fin moved downstream as the chord length decreases from 70mm to 50mm. Further, the shock terminated on the expansion wave from the tailing edge resulting cyclic wave shape in the downstream as we can see clearly for the chord

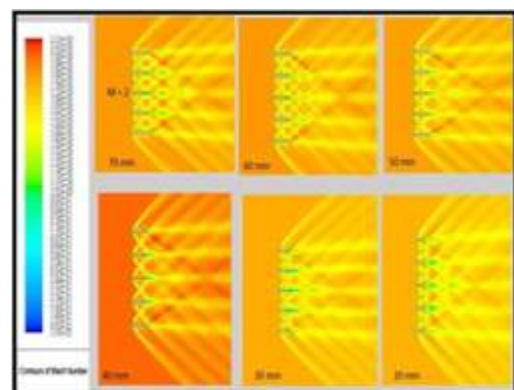


Figure 17: Parametric Study for 2D Plates at Mach 2

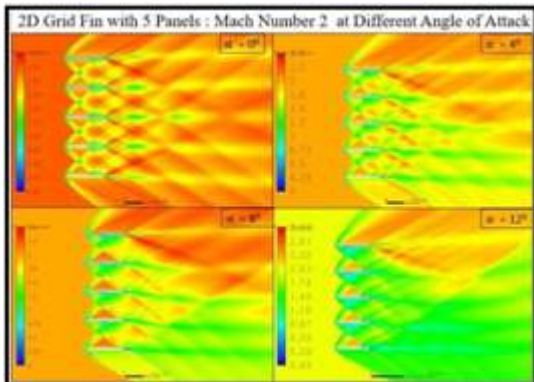


Figure 16: AOA Study for 2D Plates at Mach 2

At 0° angle of attack, the downstream flow experiences the periodic regimes containing expansion waves emanating from the top surface of the grid fin trailing edge interact with another expansion wave from the bottom surface of the upper plate. As the incidence angle increased to 4° this regime changes within the flow in downstream direction. At the higher incidence angles this periodic regime totally disappears and there is appearance of a separation bubble engulfing the whole of the upper surface of the bottom most plate.

This upper surface of the bottom most plate which does not experience a pressure relaxation at the trailing edge because of an oncoming expansion wave (unlike other plates). This event marks the onset of the separated flow regime. Once this bubble appears, within few degrees of increase in incidence, the upper surface of all the plates above are engulfed by massive separation bubble. This will be marked by an apparent stall in the lift.

Results for Freestream Mach Number 2

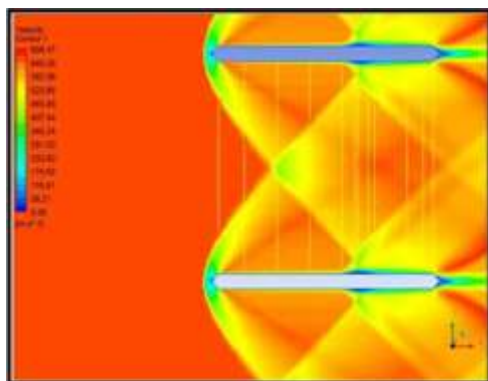


Figure 19: Data Extraction Methodology at Different Stations in 2D Grid Fin Section

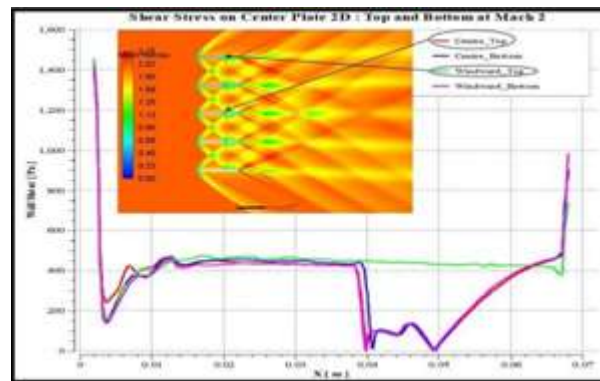


Figure 18: Mach 2 Wall Shear Distribution Different Stations for Chord length 70mm

The Yellow straight lines between the plates represent the data extraction methodology. Stations were determined along the chord length at different locations from the leading edge to trailing edge excluding the sharp boat tail and nose positions. The gap length between the two plates is 66mm from the wall to wall distance. The straight lines were discretised into 1000 points in the Fluent data (Fine grid was constructed) containing velocity values and position values plotted for analysis. The velocity profiles at different stations can be seen from the Figure 12 and Figure 21 at two different Mach numbers 0.8 and 2 respectively.

Velocity profiles at the different stations namely 2mm, 10mm, 20mm, 30mm, 40mm, 50mm, 60mm, 65mm, 68mm were chosen on the surface of the plates (Grid fin 2D section). These velocity profiles were can be seen from the Figure 21 for the freestream Mach number 2. Same stations were kept constant for remaining Mach number flows.

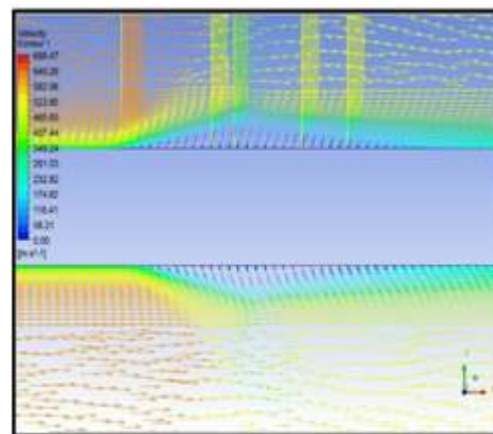
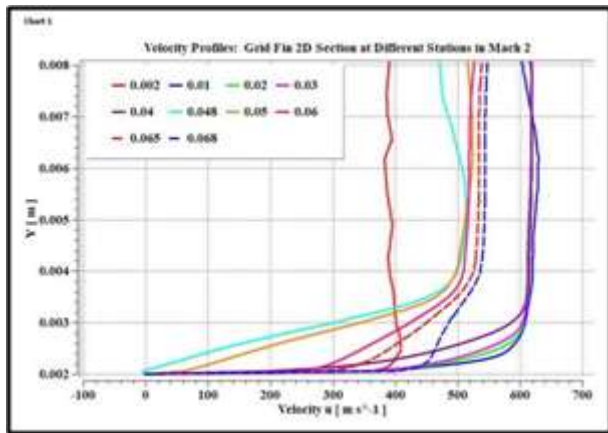


Figure 21: Separation Zone in Mach 2 Flow





**Figure 20:** Mach 2 Velocity Profiles at Different Stations for Chord length 70mm

Discussion for Viscous Flow between the 2D Grid Fin section of Five plates for an incidence angle  $0^\circ$ , It can be observed from **Figure 17** downstream flow experiences the periodic regimes containing expansion waves emanating from the top surface of the grid fin trailing edge interact with another expansion wave from the bottom surface of the upper plate clearly indicating that there was no single plate region as it was explained in the (Krishnamurthy et al., 2013). This is due to the chord length and gap length (geometrical parameters) is different. The attached shock wave emanating from the leading edge of the fin windward side of the second plate coalesces with the attached shock wave emanating from the leeward side of the first plate. This can also be observed from the CFD analysis. Further Flow continuous to expand in order to maintain the flow conditions (specified boundary conditions) downstream. Of particular interest is the complex flow structure near the trailing edge involving shock shear layer expansion wave interactions. Typically, in case of the plates of zero thickness this regime is marked by the expansion waves in (Krishnamurthy et al., 2013).

Numerical simulation for the effect of angle of attack on the grid fin 2D section for the chord length 70mm in Mach 2 has been carried out. From **Figure 17** it can be interpreted that as the angle of attack increases the bottom plate in leeward direction experiences the formation of cusped shock regime. As one particular interest in this simulation was these cusped regions were confined to top surface of the plates only. Bottom surface of the plate experiences the advancement of the normal shock from the bottom plate.

Flow separation has been observed at the reflected shock (from the shock-shock interactions) which impinges on the shear layer of the chord after the half-length at 30mm. Further this has been verified with the velocity vector and velocity profile data **Figure 20** and **Figure 21**. For the freestream Mach number 2, and Chord length 70 mm, Shock-Shock-Shear Layer interactions started from 45 mm to 48 mm which can be seen from **Figure 21** with velocity profiles in the separation. It has been observed that the presence of thick layer consisting of high reverse flow region strongly holds the upstream shock interactions. Shear stress distribution profiles on the surface of the wall gives enough confidence to confirm the flow separation location. Further, decrease in the chord length the region of the high reverse

flow shifts into the downstream direction and further it diminishes within the flow. As the freestream Mach number increases, it was observed that the leading-edge shock freely moves to downstream without any interactions with the presence of the body (Krishnamurthy et al., 2013). Decrease in the chord length results in presence of strong shock interactions followed at the downstream with shock-shock and expansion waves from the trailing edge in which these complex phenomena act as strong obstruction to the flow following wave patterns observed in **Figure 16**.

### Results for Free Stream Mach Number 2 3D Grid Fin Single Cell

The velocity profiles were plotted at different locations (stations) in the corner region of the grid fin cell. The velocity profiles provided the idea of the boundary layer thickness based on the local velocity in the station. The nature of the velocity profiles disturbed in the Mach numbers 1.2, 2, 2.5 and 3. The reason for this flow phenomenon is presence of the reflecting waves inside the cell created the discontinuities in the station data which contains the velocity and normal distance from the wall (surface of grid fin). The flow in the 3D grid fin is in complex nature and similar to the pipe flows where dominated by the pressure gradients. Basic flow features which are shock structure in the leading edges and expansion waves in the trailing edge, shock-shock interaction with the boundary layer edge, flow separation features almost same as in the 2D analysis. However, the magnitude of the shear stress, boundary layer growth, displacement thickness and momentum thickness were higher in value for the 3D Grid fin single cell corner region. For example, in 2D grid fin section at station 3 which was located at a distance of 20mm from the leading edge. For given local maximum velocity in the station 3 in freestream Mach number 0.8 the boundary layer thickness based on the maximum edge velocity it was found out that 2.8mm and the calculated displacement thickness (Eqn. 1) was 0.16mm and the calculated momentum thickness (Eqn. 2) was 0.09mm. However the results in the corner section of the 3-D Grid fin single cell having boundary layer thickness around 5-6 mm and the displacement thickness was 4.7mm, momentum thickness was 2.2mm. Compressible effects are included in the calculation of the displacement thickness and momentum thickness by considering the density values in the elemental points along the station.

The separation zone inside the 3D Grid fin single cell moves downstream as the freestream Mach number increases. It can be seen in the **Figure 22**, Flow in the grid fin cell corner section at supersonic Mach numbers 1.8, 2, 2.5 and 3. The strength of the shock wave located at leading edge increases as the freestream Mach number increases. In Mach number 1.8, it was observed that there is no separation zone inside the cell except at the leading edge and trailing edge. As the Mach number increases to 2 it can be observed that the small blue region full of recirculation of flow due to the Shock impinge on the boundary layer creating the pressure differences before the impinging zone. This complete phenomenon explained in the 2D case which illustrated from the **Figure 21**. 2D CFD results provided enough confidence by comparing the results of 2D with the corner section of the single grid fin cell (3D). Further this separation zone moved to downstream in the

Mach 2.5 and further moved downstream in the trailing edge of the corner section of the grid fin single cell in Mach 3. From this result it can be interpreted that these particular geometrical parameters containing the reflecting wave patterns inside the grid fin for the Mach numbers 2 and 3. Beyond the Mach 3 it can be assumed that the grid fin may not contain the reflecting wave patterns due to fact that in Mach 3 the reflected shock hit at the trailing edge of the grid fin cell which can be seen in **Figure 22**. For the Flows until Mach 2 development of the shock in front of the leading edge which allows to maintain constant mass flow rate along the grid fin section due to the development of the boundary layer growth. As the Mach number increases the boundary layer growth decreased and comes close to the surface of the grid fin.

Further these separation regions were verified with the shear stress distribution on the surface of the grid fin section. The shear stress becomes zero at the point of the separation which can be seen in the **Figure 26**.

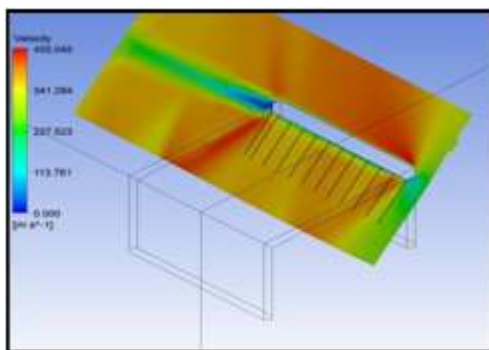


**Figure 23:** Corner region of an 3D single cell and data extraction methodology

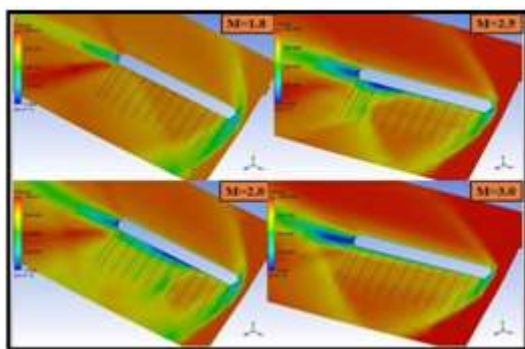


**Figure 22:** Velocity Contours in Different

Freestream Mach Number Flows in Grid Fin Cell (Low supersonic to Supersonic region  $1.8 < M < 3$ )

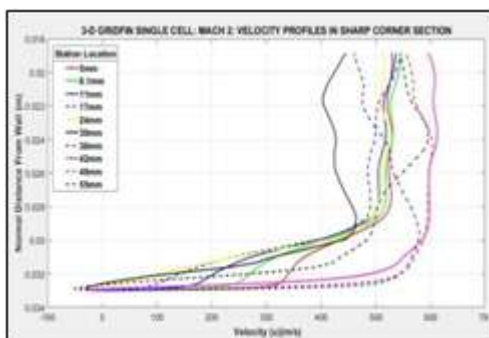


**Figure 25:** Velocity Profiles at Corner Section of an 3D Grid

fin single cell for Mach 2

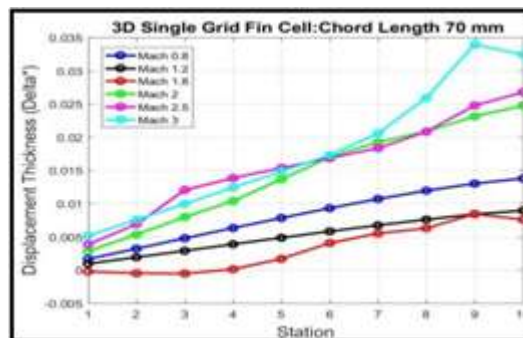


**Figure 24:** Displacement Thickness growth in Corner Section of Grid Fin

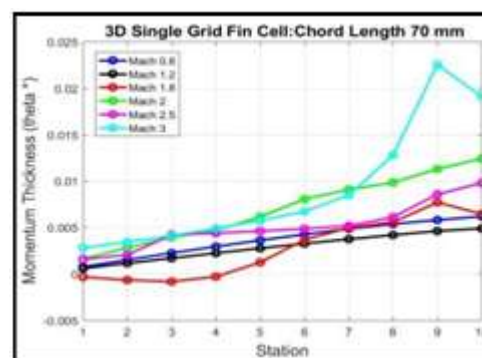


**Figure 27:** Momentum Thickness growth in Corner Section of the Grid Fin

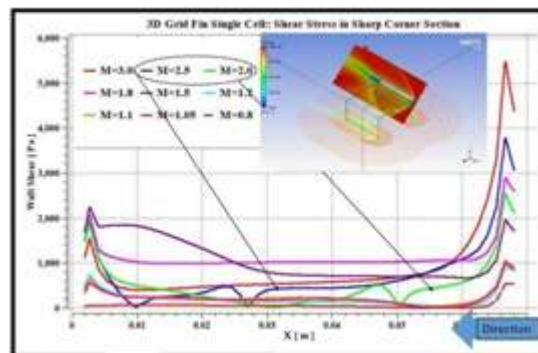


**Figure 26:** Wall Shear Distribution in Corner region of 3D Grid Fin Cell

### 5. Conclusion

The purpose of this work is incorporate the CFD analysis of Viscous flows in the sharp corner of the grid fin cell at free stream Mach numbers 0.8, 1.2, 2, 2.5, 3. 2D CFD analysis carried out to understand the basic flow features like shock interactions, shock- shock interactions, shock-shock-boundary layer interactions, flow separation region in the grid fin cells by considering the cross-sectional section by keeping the geometric parameters constant.

Basic analysis carried out at free stream Mach number 2. Further research work needs to carry out for the entire grid fin with 25 cells to calculate the interference effects on the individual cells. The grid fins are having potential to perform as at least as the planar fins in supersonic Mach numbers. Transonic Mach number performance also possible by careful design considerations. Extensive research work



currently carrying on Grid fins due to its feasibility in the aerobraking and control mechanism in supersonic speeds. Grids fins with curved shape, with spikes, no of grid fins etc are current research area in this field.

The boundary layer growth in the sharp corner of the grid fin cell calculated with the velocity profiles at different stations. Flow separation zone had been identified for the current configuration and explained the flow physics about it. Different type of flow regimes explained by considering the 2D grid fin model

The outcome of the present work can be used to identify the Mach number regions where the shock impinges on the surface of the grid fin and Mach number in which grid fin cell is free from the shock impingements., displacement thickness and momentum thickness has been calculated for the 3-D geometry and plots has been done at various Mach numbers. High angle of attack behaviour of the grid fin was investigated to characterize the linear response range in Mach numbers from 0.8 to 3

Following research items are addressed as future work:

A similar design procedure is planned to be applied for low and high supersonic regimes for full scale grid fin.

- 1) The sample design in current thesis study constitutes an aerodynamic database for changing parameters within certain geometric restrictions. This database is planned to be enlarged considering different geometric and structural restrictions. The design procedure is planned to be applied on various missile body types possessing different static stability characteristics.
- 2) Roll control characteristics and their effect on the design of the grid fin should also be covered in the future. Frame profile is one of the items that is not covered in current thesis. It is also important parameter in decreasing drag force as well as being a structural member. Therefore, its optimization should be addressed in the future.
- 3) Lengths of the connecting rods are also one of the parameters that is not studied in this thesis. Determination of this parameter is also planned to be studied in the future.

## 6. Acknowledgement

The Authors acknowledging the Computational Facility provided by the Vikram Sarabhai Space Center, Trivandrum, India.

## References

- [1] G. Abate and R. Duckerschein. Subsonic/transonic free-flight tests of a generic missile with grid fins. In 38 th AIAA Aerospace Sciences Meeting and Exhibit, AIAA-2000-0937, Reno, NV, USA, January 2000.
- [2] G. Abate, G. Winchenbach, and W. Hathaway. Transonic aerodynamic and scaling issues for lattice fin projectiles tested in a ballistic range. In 19th International Symposium of Ballistics, Interlaken, Switzerland, May 2001
- [3] S. M. Belotserkovsky, L. A. Odovol, Y. Z. Safin, A. I. Tylenov, V. P. Frolov, and V. A. Shitov. Reshetchatye Krylya (Lattice Wings). Mashinostroenie, Moscow (in Russian), 1985.
- [4] J. E. Burkhalter and H. J. Frank. Grid fin aerodynamics for missile applications in subsonic flow. *Journal of Spacecraft and Rockets*, 33(1), January-February 1996.
- [5] Debiasi, M., Zeng, Y., and Chng, T. L., 'Swept-Back Grid Fins for Transonic Drag Reduction', AIAA Paper 2010-4244, June 2010
- [6] Dikbas Erdem (2015) 'Design of A Grid Fin Aerodynamic Control Device For Transonic Flight Regime'
- [7] E. Dikbaş, Özgür Uğraş Baran, and C. Sert. A 2-D theoretical and computational study for preliminary determination of grid fin geometric parameters at low transonic speeds. In 7th Ankara International Aerospace Conference, AIAC-2013-049, Ankara, Turkey, September 2013.
- [8] M. C. Hughson and E. L. Blades. Transonic aerodynamic analysis of lattice grid tail fin missiles. In 24th AIAA Applied Aerodynamics Conference, AIAA-2006-3651, San Francisco, CA, USA, June 2006.
- [9] R. W. Kretschmar and J. E. Burkhalter. Aerodynamic prediction methodology for grid fins. In RTO AVT Symposium on "Missile Aerodynamics", pages 11-1-11-11, Sorrento, Italy, May 1998
- [10] K. S. Orthner. Aerodynamic analysis of lattice grid fins in transonic flow. Master's thesis, Air Force Institute of Technology, 2004
- [11] Ravindra K, Nikhil V. Shende and Balakrishnan (2013), 'CFD Simulation of the Grid Fin Flows' 31st AIAA Applied Aerodynamics Conference, 24-27 June 2013, San Diego, California
- [12] Y. Zeng, J. Cai, M. Debiasi, and T. L. Chng. (2009) Numerical study on drag reduction for grid-fin configurations. In 47th AIAA Aerospace Science Meeting Including The New Horizons Forum and Aerospace Exposition, AIAA-2009-1105, Orlando, FL, USA, January 2009
- [13] Wm David Washington, Mark S Miller, 'Experimental Investigations of Grid Fin Aerodynamics: A Synopsis of Nine Wind Tunnel and Three Flight Tests', AIAA, 1994.
- [14] G. Abate and R. Duckerschein. Subsonic/transonic free-flight tests of a generic missile with grid fins January 2000. In 38 th AIAA Aerospace Sciences Meeting and Exhibit, AIAA-2000-0937, Reno, NV, USA
- [15] E. Dikbaş, Özgür Uğraş Baran, and C. Sert. A 2-D theoretical and computational study for preliminary determination of grid fin geometric parameters at low transonic speeds, September 2013. In 7 th Ankara International Aerospace Conference, AIAC-2013-049, Ankara, Turkey